A multiscale point of view on the dynamics of stably stratified turbulence associated with geostrophic modes: simulations and model

F.S. Godeferd[*], A. Delache, L. Gostiaux & C. Cambon

Fluid Mechanics and Acoustics Laboratory UMR 5509 CNRS
École centrale de Lyon, Université de Lyon, Université Jean Monnet Saint-Étienne
France
[*] Corresponding author: fabien.godeferd@ec-lyon.fr

Abstract

We study the dynamics and horizontal layering of homogeneous stably stratified turbulence (SST) from the point of view of two-point correlation spectra. We retain the most complete spectral description that is available in this axisymmetric setting, by computing the angular-dependent spectra, so that we observe the *anisotropy of the flow at each scale* — that is at a given wavenumber — and for each orientation of the wavevector — this corresponds to a given direction of separation of the two-point correlation. Moreover the flow is decomposed into geostrophic and ageostrophic motion, in other words waves and vortex contributions[14] also denoted toroidal/poloidal.[4] This complete statistical setting therefore permits to study the interplay between waves and turbulent motion in different regimes of stably stratified turbulence, characterized by the Reynolds and Froude non dimensional numbers. From results of high resolution Direct Numerical Simulations and of a statistical model of freely decaying SST, we observe that the spectral characterization of the flow structure brings to light the relevance of the Ozmidov scale for separating scales which are strongly affected by the buyoancy force, although we also show that a refined analysis of the anisotropic dynamics requires modal decomposition.

1 Introduction

Stably stratified homogeneous turbulence (SST) exhibits quasi-horizontal structures organized in vertically sheared layers, as shown long ago by in situ observations [17], in laboratory experiments [10] and in direct numerical simulations [2] (DNS) (See Fig. 1). The thickness of these layers seems to scale according to a unit value of a related Froude number (see *e.g.* [16, 18]). However, at smaller scales, turbulent structures apparently recover an isotropic state. In this context, Ozmidov introduces a length scale $l_O = (\varepsilon/N^3)^{1/2}$ [12], where N is the Brunt-Väisälä frequency [$N = (gd\rho/dz)^{1/2}$ with ρ the mean density gradient and g the gravity] and ε the dissipation. This scale is defined by stating the equilibrium between inertial and buoyancy forces, also quantified by the Froude number $Fr^l = v/Nl$ (with v the velocity of a structure of size l): structures larger than l_O ($Fr^l \ll 1$) are strongly influenced by stratification whereas structures smaller than l_O ($Fr^l \gg 1$) recover three-dimensional isotropy (see schamtic in Fig. 7-left). The Ozmidov scale is therefore useful for characterizing the regime of SST in numerical simulations [11, 1] or in experiments [15, 8]. In addition, theoretical models are also available for SST, several of which rely on a length- and time-scale separation of velocity field $\mathbf{u}$ between the geostrophic motion and the ageostrophic motion [13]:

$$\mathbf{u} = \underbrace{\nabla_h \times \psi}_{\text{vortex}} + \underbrace{\nabla_h \zeta + u_z \mathbf{z}}_{\text{wave}}$$
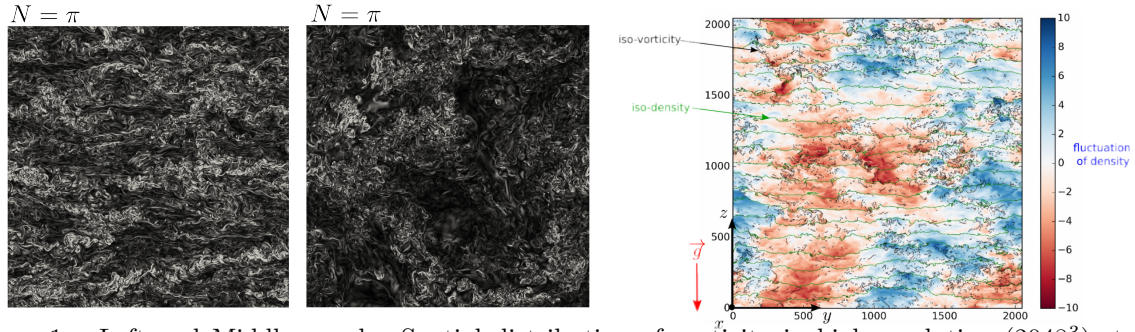
Figure 1: Left and Middle panels: Spatial distribution of vorticity in high resolution (2048^3) stably stratified turbulence DNS. $N = \pi$ is the Brunt-Väisälä frequency, here corresponding to moderately small Froude number of order 0.1. *Left*: horizontal plane cut; *Middle*: vertical plane cut. One clearly observes both strong horizontal motion and vertical layering, as well as large-scale anisotropy and small-scall more isotropic "worms", corresponding to the difference of energy among scales and orientations presented in Fig. 3 spectra. *Right panel*: Visualization of the 2048^3 DNS field in a vertical plane of strongly stratified turbulence: isodensity fluctuations are shown in color. Isovorticity lines are shown in black, and isolines of total density in blue.

($\mathbf{z}$ is the unit axis that bears gravity) but very few address explicitly the geostrophic/ageo-strophic modal decomposition dependence with the scale which is considered. This decomposition for homogeneous stably stratified turbulence may also be called toroidal/poloidal [4] or vortex/wave, [14] and is performed in spectral space by an algebraic projection of the Fourier-transformed velocity field onto the Craya-Herring frame of reference [5, 9].

We propose here to study the scale-by-scale anisotropy of SST using spectra of two-point velocity correlations focusing on the dynamics that creates anisotropy at different scales. We especially focus on the vortex/waves decomposition of energy spectra and their related spectral transfers, and especially on their dependence on the scale or wavenumber k and orientation θ_k of the wavevector with respect to gravity axis (assuming axisymmetry, therefore no azimuthal dependence).

Important questions we address in this work are: What is the anisotropic distribution of energy (scales and direction) at large scales, and what are the relative amplitudes of kinetic energy of vortex, waves and potential energy? How does the flow recover isotropy in terms of its dynamics at smaller scales and is the Ozmidov scale relevant? What are the relative contributions of geostrophic modes *non linear* interactions with respect to those involving ageostrophic modes in the energy transfer $T(k, \theta_k)$ at different scales (where θ_k is the orientation *w.r.t.* gravity)?

In order to discuss these questions and provide some answer to them, we have performed high resolution DNS (2048^3) varying the Froude number so that the Ozmidov scale lies either within the inertial spectral range or is much smaller than all the scales of the flow (all scales anisotropic), so that we reproduce the dynamics of turbulence partially or fully affected by stratification (in terms of length scales). The modal geostrophic/ageostrophic decomposition is achievable in the corresponding velocity fields, and energy transfers can be extracted. We compare the obtained statistics to results of a two-point statistical model (EDQNM model, see [7]) that permits to reach Reynolds number regimes and above, and moreover provides a refined analysis of the basic modal interactions (geostrophic-mode-related or ageostrophic-mode-related) that constitute the complete energy transfer. These refined decompositions are very hard to achieve even in modern state-of-the-art DNS, by lack of statistical sampling after decomposition of the velocity statistics in scales/angles/modes/contributions.

We also use the two-point statistical spectral model of EDQNM type to investigate the spectral anisotropy of SST with extended infrared, inertial and viscous ranges in order to evaluate the presence of very large scale dynamics. Such a refined characterization of SST in the homogeneous case is important for the estimate of mixing efficiency, as studied experimentally in the paper by Micard *et al.* in the present ISSF 2016.

2   SST flow structure and overall dynamics

From initially isotropic turbulence in which density is a passive scalar, we apply stratification by turning on gravity, and then let the flow decay under the action of viscous dissipation and buoyancy force. The initial Froude numbers for the different simulations vary between 10^{-1} and 10^{-3} for N varying between 3.1 and 25.1, and the Reynolds number is of order 1000 in these high resolution 2048^3 DNS. Fig. 2-left shows the typical evolution of kinetic energy with two essential features: (a) the larger the stratification, the slower the decay with respect to the reference isotropic case at $N = 0$; (b) strong oscillations appear due to the exchange of energy between waves kinetic energy and their potential energy, as a sign of the large-scale vertical oscillating motion. These features also appear on the predictions of the EDQNM statistical model for kinetic, horizontal and vertical energies in Fig. 6-left. Accordingly, the kinetic energy spectra shown in Fig. 2-right show a slight departure of the SST spectra from the $k^{-5/3}$ Kolmogorov scaling.
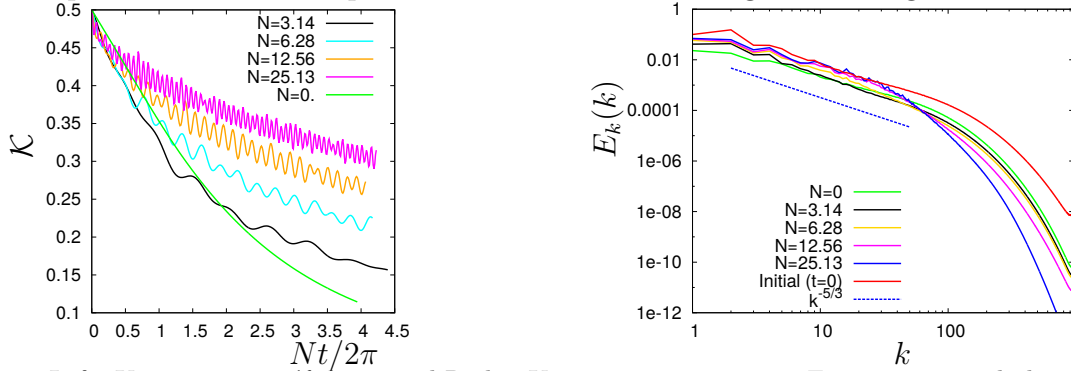

Figure 2: Left: Kinetic energy $\mathcal{K}$ decay and Right: Kinetic energy spectra. For isotropic turbulence and for stably stratified turbulence at four different values of the Brunt-Vaisala frequency N. (2048^3 DNS data)

3   Relevance of Ozmidov scale as parameter of two-point correlation spectra anisotropy

In kinetic energy spectra, the Ozmidov scale l_O is expected to indicate a separation between a large-scale spectral range which is strongly affected by stratification and is thus rendered anisotropic, from a smaller-scale spectral range in which the flow starts to recover a more isotropic energy distribution. Consistently with this scale complexity, observations of the spatial distribution of vorticity in Fig. 1 shows large-scale features resembling that of two-dimensional turbulence in the horizontal plane, whereas smaller three-dimensional vortex filaments are observed. Fig. 3 shows the different kinetic energy *density* spectra $E(k, \theta_k)$. First, note that they retain the directional dependence with the orientation of the wavevector, whereas kinetic energy spectra of Fig. 2-left shows spherically integrated spectra, thus discarding the explicit θ_k dependence. The two bottom panels of Fig. 3 show that in the initial condition, or later in the unstratified decay, energy density spectra in

all directions collapse. However, when stratification is present, the energy density spectra for horizontal wavevectors retain much less energy than those for vertical wavevectors, consistently with the fact that the flow organizes in strong horizontal layer with more energy in the horizontal motion than in the vertical one. Note also that the larger the stratification, the larger the departure. However, this departure is not uniform in scales, so that for the least stratified cases at $N = \pi$ and 2π, the small scales of the density spectra are very weakly anisotropic with respect to the large scales. The location of the transition range is clearly marked by the Ozmidov wavenumber $2\pi/l_O$ which is indicated by a vertical line in the figures. Note also that the isotropic recovery is not merely due to viscosity, since it very clearly occurs within the inertial spectral range in the $N = \pi$ case. Finally, in the mostly stratified case at $N = 8\pi$, spectra are anisotropic even in the dissipative range. This is due to the fact that the Ozmidov wavenumber is larger than the largest wavenumber (smallest scale) resolved in the flow.

However, one has to consider the fact that in decaying SST the length scales evolve in time, and we observe for instance in Fig. 7-right from long-time EDQNM evolution that while the integral and Kolmogorov lengths increase due to the self-similar decay (from $t \simeq 0.5$, after the initial transient), the Ozmidov length itself decreases rapidly, and crosses first the integral scales, then the Kolmogorov scale, so that at large times all the flow scales are affected by stratification. The role of Ozmidov scale in SST is similar to that of the Zeman scale $(\varepsilon/\Omega^3)^{1/2}$ in rotating turbulence, in which the Zeman scale also separates anisotropic large scales from more isotropic smaller scales, with a rather smooth transition [6]. This is very different from the situation of unstably stratified homogeneous turbulence, in which the Ozmidov scale can be defined similarly as in SST, and in which it appears as a sharp cut-off scale between strongly anisotropic infrared spectral range and almost immediately fully isotropic inertial and viscous spectral ranges [3].

4   Modal anisotropy: kinetic, potential, vortex, waves

We propose here a refined study of anisotropy in the flow, based on the different modal energies that are present, in order to provide a better understanding of the dynamics of the flow that creates the specific layering. On the one hand, kinetic and potential energy exchanges occur at all scales, from vertical oscillations due to the presence of internal gravity waves. On the other hand, the vortex motion exchanges energy with waves, in a rather complex way.

We first study the scale-by-scale distribution of kinetic and potential energies in Fig. 4, and more specifically the potential to kinetic ratio $E_p(k)/E_k(k)$ as a function of wavenumber. At large scales (small k), there is an equipartition between the waves kinetic and potential energy, and, since waves and vortex have similar kinetic energy, the ratio is of order 1/2. Further down the scales, at large k, we observe an increase of the ratio, indicating that potential energy of the small scales is larger than their kinetic energy. This effect seems however to be partially due to the structure of scalar variance spectrum in the dissipative ranges (here the Prandtl number if of order one), from the curve at $N = 0$. There is nonetheless a clear dependence of the ratio with N. Overall, inertial and dissipative ranges behave differently from the point of view of potential to kinetic energy equilibrium. We now study the ratio between potential and waves energy density $E_p(k, \theta_k)/E_w(k, \theta_k)$ in Fig. 5-left and the ratio between potential and vortex energy density $E_p(k, \theta_k)/E_v(k, \theta_k)$ in Fig. 5. The two distributions of these ratios are very different. Accounting for the unavoidable jitter in the curves due to lack of sampling of DNS in
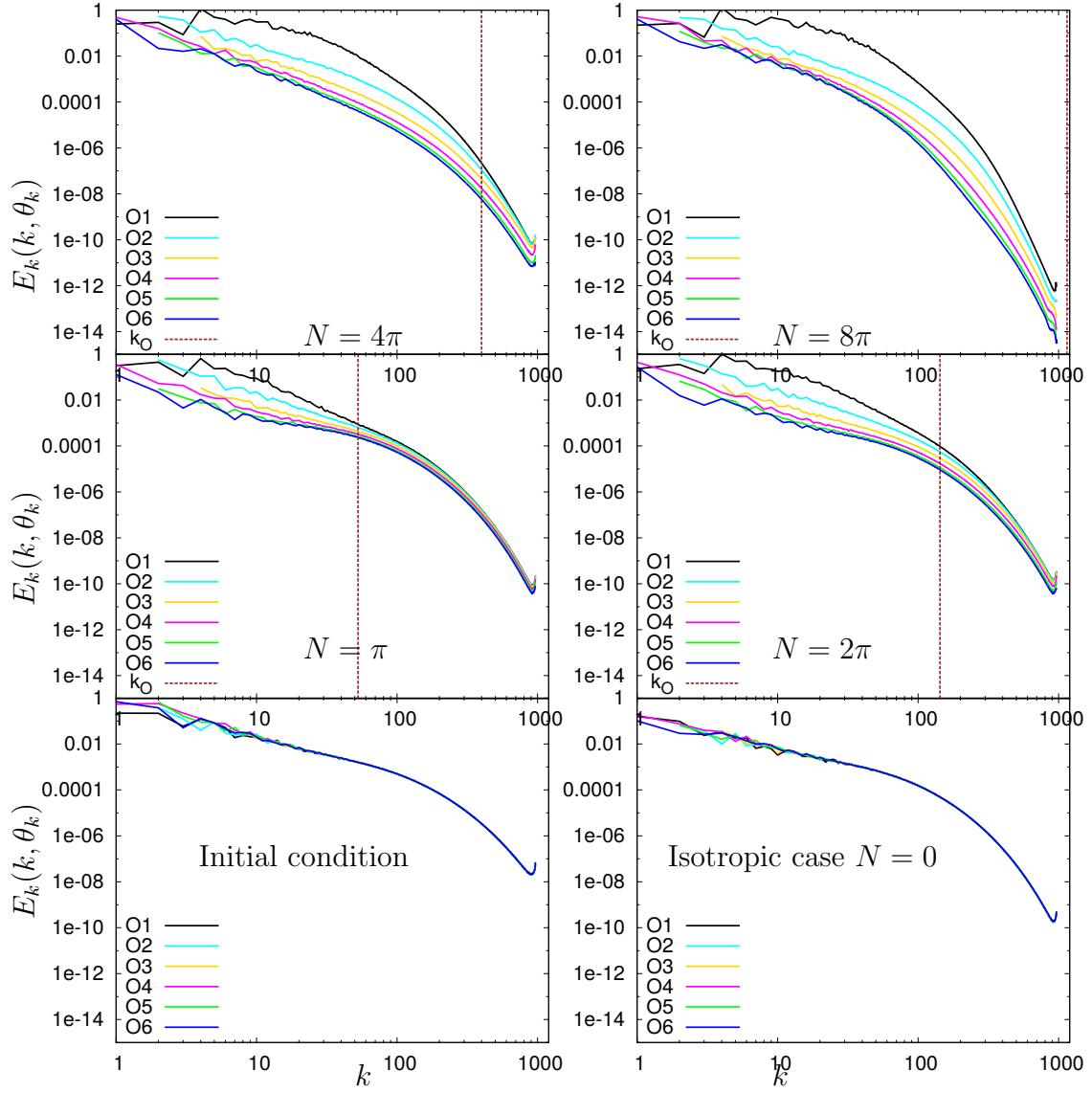
Figure 3: Spectral kinetic energy density distribution $E_k(k, \theta_k)$ for wavevector oriented from vertical (label O1) to horizontal (label O6). 2048^3 DNS of stably stratified homogeneous turbulence. From left to right and bottom to top, the figures show: the initial condition, the isotropic reference case at $N = 0$, increasing stratification $N = \pi$, 2π, 4π, 8π. The vertical dashed line shows the Ozmidov wavenumber $(N^3/\varepsilon)^{1/2}$.

the large scales, it seems that the first figure shows a dominance of potential energy over vortex energy in the large scales and in horizontal spectra, but this trend is reversed in the smaller scales, with a strong increase of potential energy in vertical spectra at small scales. This accounts for the above-mentioned increase of potential energy over total kinetic energy in spherically averaged spectra in Fig. 4. Indeed, Fig. 5-right for E_p/E_v shows only a very weak dependence of this ratio with θ_k at small scales, whereas it is strongly dependent on orientation at large scales. Overall, one concludes that the dynamics of the flow in terms of modal energy exchanges depends significantly on the observed scale, but the Ozmidov wavenumber which is indicated in Fig. 5 gives an order of magnitude of the separation, unlike a rather clear separating wavenumber $k \simeq 30$ observed in Fig. 5-right.
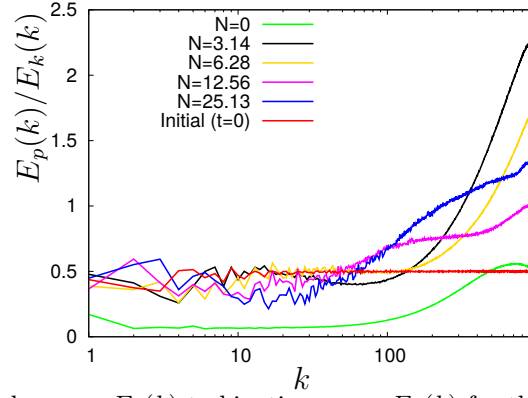
Figure 4: Ratio of potential energy $E_p(k)$ to kinetic energy $E_k(k)$ for the initial condition, the isotropic run, and the four stably stratified runs of turbulence. (2048^3 DNS data)
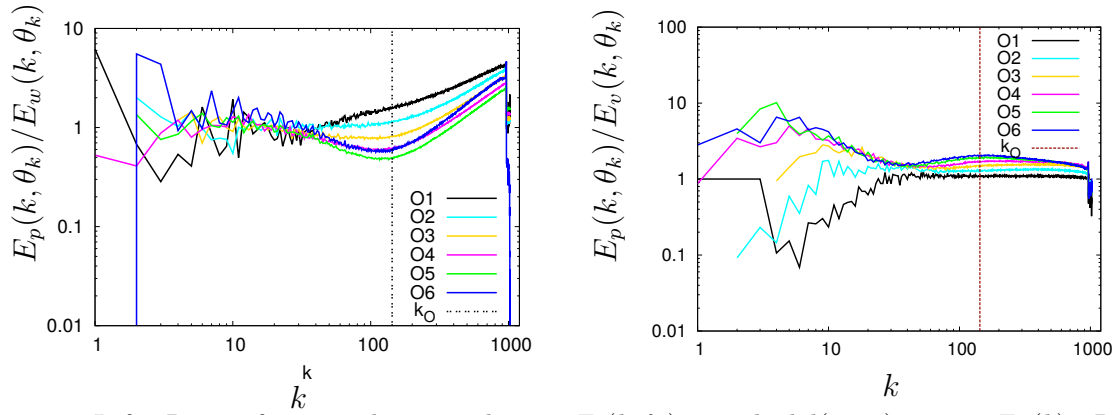

Figure 5: Left: Ratio of potential energy density $E_p(k, \theta_k)$ to poloidal(wave) energy $E_w(k)$. Right: Ratio of potential energy density $E_p(k, \theta_k)$ to toroidal(vortex) energy $E_v(k)$. For the initial condition, the isotropic run, and the four stably stratified runs of turbulence. O1 for vertical-most wavevectors, O6 for close to horizontal ones. (2048^3 DNS data)

5 Lessons learned from a two-point statistical model (EDQNM-type)

The EDQNM model is a two-point statistical model which solves equations for the two-point velocity-density correlation spectra using a quasi-gaussian closure. It was shown to compare very well with DNS of SST in parametric ranges common to the two approaches (see *e.g.* [18]). The advantages of the model is that: (a) it permits to reach a wider range of parameters, especially the Reynolds number; (b) it provides smooth spectra and thus is not subject to the large statistical uncertainties at large scales that are present in DNS, unless one would pay the price for ensemble averaging; (c) the flow evolution is not subject to physical box confinement, since a very wide spectral range can be chosen.

5.1 Energy evolution and spectra

As mentioned above, Fig. 6-left shows results from EDQNM for energetics of decay of SST in agreement with DNS ones. Although we do not present here the exact same parametric cases as for DNS, Fig. 6-right shows kinetic energy density spectra that exhibit a similar anisotropic distribution as in DNS in the inertial range. Spectra at two times are presented in the Figure, in order to emphasize a particular feature that was not observable in DNS due to limited box size: while the anisotropy in the spectra develops in the inertial range (and eventually in the viscous sub-range depending on the intensity of stratification),
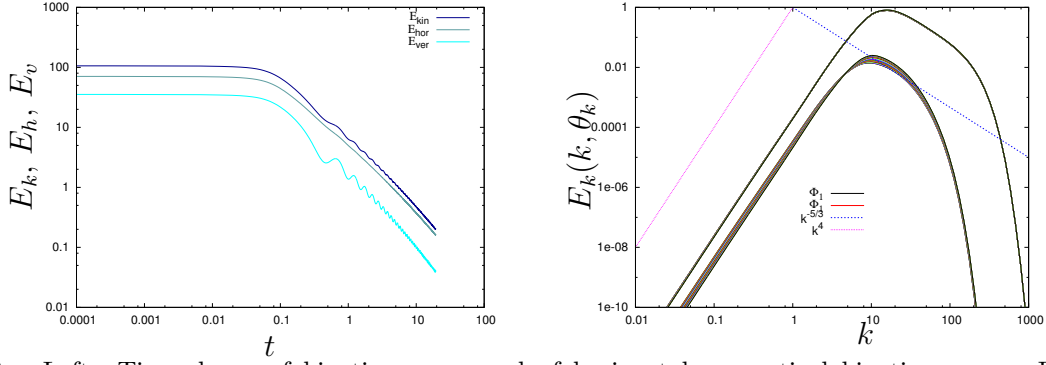
Figure 6: Left: Time decay of kinetic energy and of horizontal an vertical kinetic energy. Right: Toroidal(vortex) energy density spectra at time $t \simeq 0.1$ (top spectrum) and time $t \simeq 0.25$ (bottom spectrum, shifted by one decade down for clarity). (EDQNM model data)
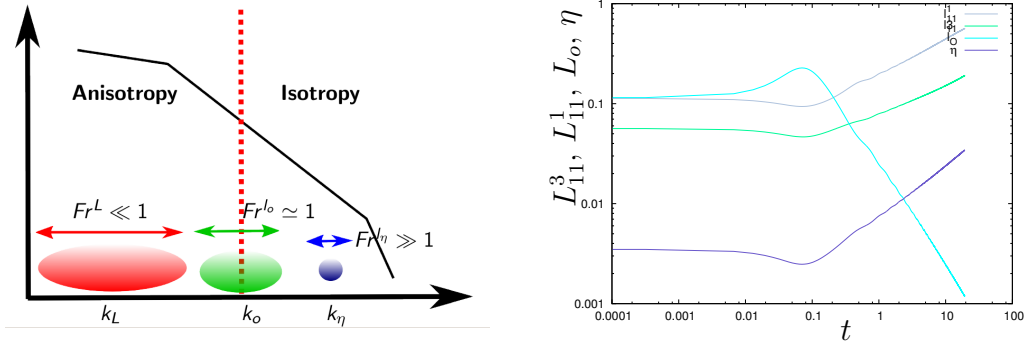

Figure 7: Left: Schematic of the relative position of the different wavenumbers associated with the integral length scale, the Ozmidov scale and the Kolmogorov dissipative length scale. Right: Time evolution of the corresponding length scales in freely decaying stably stratified turbulence (note that the integral length scale obtained from two-point velocity correlations of horizontal velocity with vertical (L_{11}^3) and horizontal separation (L_{11}^1) are shown rather than the global one that is an average of the two). (EDQNM model data)

the infrared spectrum also becomes significantly anisotropic, as a trace of the influence of the buoyancy force on the largest scales of the flow. There is however no noticeable backscatter, since the slope of the infrared spectrum is preserved. Observing the infrared anisotropy up to the largest scales (smallest wavenumbers) suggests that in real SST, the mean stratification gradient will also evolve in time due to nonlinear turbulent mixing.

5.2   Energy transfers

We show in Fig. 8 the transfers that can be obtained from EDQNM model, including transfers of modal energies, potential, waves and vortex kinetic energy, but EDQNM also gives access to separate contributions in these transfers from vortex, waves, or mixed vortex-waves interactions. The left panel of the figure shows the global kinetic energy transfer $T^K(k)$, with a scale distribution similar to that of isotropic turbulence: a direct energy cascade is shown by a negative transfer in the inertial range and positive transfer in smaller wavenumbers. The figure also shows the anisotropic distribution of the vortex kinetic energy density transfer $T^V(k, \theta_k)$, but with an overall shape which is close to that of T^K, corresponding to a mostly downscale transfer of energy. Its dependence on θ_k is consistent with the observed anisotropy in energy density spectra.

What EDQNM adds to our understanding of the dynamics of SST, is the contribution of purely vortex interactions to T^V, plotted in Fig. 8-right. This energy transfer is mostly

between different directions, and corresponds to a *directional* energy redistribution (from horizontal to vertical wavenumbers, see arrow on the figure) rather than between scales. It shows that this geostrophic "cascade" is the main cause of the vertical layering in the flow at moderate Reynolds and Froude number regimes [7, 18]. Therefore, a simplistic picture of the energy transfers in freely decaying SST at these regimes would be: (a) angular energy drain from geostrophic modes interactions, superimposed with (b) a more classical downscale cascade *à la Kolmogorov* mediated by interactions involving ageostrophic modes. In this picture, the Ozmidov scale l_O can hardly be introduced, since the transfer from purely vortex interactions on the figure do not seem to relate easily to l_O. It may therefore be necessary to introduce a directional dependence in this separating scale, for instance by proposing a vertical Ozmidov scale and a horizontal one, rather than a unique one, in models of stably stratified turbulence. This is left for future work.
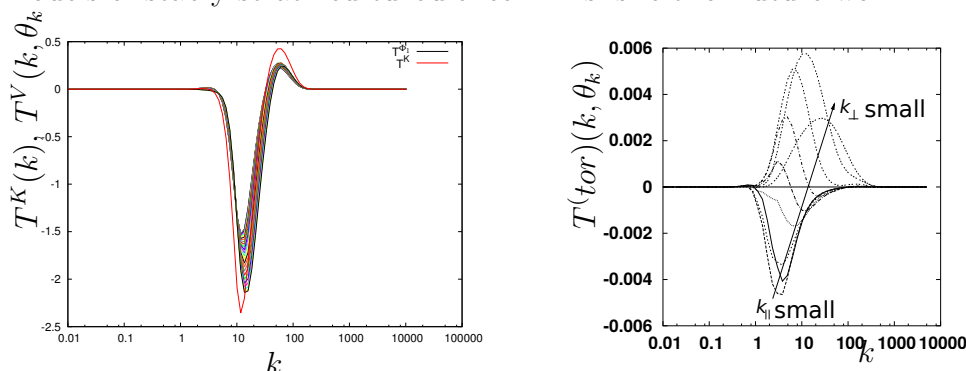

Figure 8: Left: Kinetic energy transfer $T^K(k)$ and transfer of vortex kinetic energy density $T^V(k, \theta_k)$. Right: Contribution to the vortex energy density transfer due to quadratic contributions of vortex energy density only, that is without the contribution of waves (from [7]). (EDQNM model data)

References

[1] P. Augier, J.-M. Chomaz & P. Billant , J. Fluid Mech., 713, pp 86-108, 2012

[2] G. Brethouwer, P. Billant, E. Lindborg & JM. Chomaz. J. Fluid Mech. 585, 343-368, 2007

[3] A. A. Burlot, B.-J. Gréa, F. S. Godeferd, C. Cambon & O. Soulard. Phys. Fluids 27, 065114, 2015

[4] S. Chandrasekhar, Hydrodynamic and hydromagnetic stability, Oxford, p. 622, 1961

[5] A. Craya. Contribution à l'analyse de la turbulence associée à des vitesses moyennes. P.S.T. Ministère de l'air (Paris), 345, 1958

[6] A. Delache, C. Cambon & F. S. Godeferd. Phys. Fluids 26, 025104, 2014

[7] F. S. Godeferd & C. Cambon, Phys. Fluids 6, 2084-2100, 1994

[8] H. van Haren & L. Gostiaux. Oceanography 25(2):124-131, 2012

[9] J.R. Herring. Phys. Fluids 17, 859–872, 1974

[10] J.H. Lienhard V & C.W. Van Atta, J. Fluid Mech., Vol. 210, pp.57-112, 1990

[11] R. Marino, P.D. Mininni, D.L. Rosenberg & A. Pouquet, Phys. Rev. E, 90, 2, 2014

[12] Ozmidov R.V. Izvestia Acad. Sci. USSR, Atmosphere and Ocean Physics, #8, 1965

[13] J. Pedlosky, Geophysical Fluid Dynamics, Springer, 1987

[14] J.J. Riley, & M.-P. Lelong. Ann. Rev. Fluid Mech. 32 (1), 613-657, 2000

[15] J.J. Riley & E. Lindborg. J. Atmos. Sci., 65, 2416–2424, 2008

[16] J. J. Riley & S. M. de Bruyn Kops. Phys. Fluids, 15 (7): 2047-2059, 2003

[17] F. Dalaudier & C. Sidi. J. Atmos. Sci., 44, 3121–3126, 1987

[18] C. Staquet & F.S. Godeferd, J. Fluid Mech. 360, 295-340, 1998